Hybridization Networks of mRNA and Branched RNA Hybrids

Vassiliki Damakoudi,[a] Tobias Feldner,[a] Edina Dilji,[a] Andrey Belkin,[a] and Clemens Richert*[a]

Messenger RNA (mRNA) is emerging as an attractive biopolymer for therapy and vaccination. To become suitable for vaccination, mRNA is usually converted to a biomaterial, using cationic peptides, polymers or lipids. An alternative form of converting mRNA into a material is demonstrated that uses branched oligoribonucleotide hybrids with the ability to hybridize with one or more regions of the mRNA sequence. Two such hybrids with hexamer arms and adamantane tetraol as branching element were prepared by solution-phase synthesis. When a rabies mRNA was treated with the branched hybrids at 1 M NaCl concentration, biomaterials formed that contained both of the nucleic acids. These results show that branched oligoribonucleotides are an alternative to the often toxic reagents commonly used to formulate mRNA for medical applications.

Introduction

Branched oligonucleotides are a new class of synthetic nucleic acids with interesting properties. They are made up of a branching element or core and oligonucleotide arms that can engage in Watson-Crick base pairing with complementary strands.[1] Because base pairing can occur with several partner strands in three dimensions, hybridization characteristics different from those of linear oligonucleotides result.[2–4] When small, rigid organic cores are used, DNA arms as short as dimers can suffice to drive the assembly of branched oligonucleotides into solids.[5,6] When solution-phase syntheses are employed, macroscopic quantities of hybrids can readily be obtained.[7–9] For DNA, branched hybrids with up to 32 nucleotides have been prepared in solution.[10]

Among the possible applications for branched oligonucleotide hybrids is the use in converting bioactive compounds into materials. This has been shown for branched DNA hybrids with short "zipper" arms. The hybridization networks formed by such species can capture a range of different active pharmaceutical ingredients and release them into serum from the resulting solid.[11] Further, it was recently shown that hybridization networks made up of hybrids and linear duplexes as spacers or binding sites can encapsulate proteins, either by non-specific capture upon precipitation or based on sequence-specific binding events.[12] The resulting hybrid materials can stabilize proteins against denaturation. Encapsulation and protection of sensitive biomolecules is an important issue for medical applications.

One class of biomolecules that is emerging as novel therapeutics, vaccines or gene editing agents are messenger RNAs. For example, studies on mRNA vaccines against cancer[13–16] and viral diseases,[17–21] including clinical trials aimed at SARS-CoV-2 have been initiated.[22–24] Vaccination, as well as other potential medical uses of RNA[25,26] benefit from a formulation of the labile polynucleotide chains. By itself, mRNA suffers from minimal cell penetration and stability, caused by its size, polyanionic character and lability to enzymatic degradation.[27,28] Complexation can lead to bundles of mRNAs in polyion complexes that facilitate delivery into cells.[29] More conventional transfection experiments with mRNA have been performed with cationic liposomes,[30] electroporation,[31] or a "gene gun",[32] but such approaches are not suitable for clinical applications. Instead, biomaterial- or nanoparticle-based strategies are being sought.[27] Here again, the cationic peptides, polymers or lipids commonly used to prepare the materials can be quite toxic or poorly defined on a molecular level.[27,33] This prompted us to ask whether less toxic agents that bind to the mRNA through more selective interactions could be employed to create biomaterials with the potential to be used in the clinic.

Here we report the synthesis of oligoribonucleotide hybrids with four hexamer arms that can base pair simultaneously with two different regions of mRNA molecules, acting as crosslinking agents by hybridization (Figure 1). The first has RNA arms of the sequence U_6 that can hybridize to poly(A) tails of mRNA. The other has four hexamer arms of the sequence 5′-CAUGGU-3′, which is complementary to the initiation site of translation of the mRNA chosen. The two hybrids were prepared by solution-phase chain assembly. This made their syntheses considerably less expensive than solid-phase syntheses, and easier to scale up. Solution phase syntheses also avoid issues with limiting pore sizes of non-swellable supports, such as controlled pore glass, and the steric demand of branched chains. Both RNA hybrids were found to lead to the formation of a biomaterial when mixed with mRNA designed to act as vaccine for the rabies virus.[34] The formation of the materials occurs in dilute aqueous solution devoid of divalent cations and devoid of

[a] V. Damakoudi, T. Feldner, E. Dilji, A. Belkin, Prof. C. Richert
Institute of Organic Chemistry, University of Stuttgart
70569 Stuttgart (Germany)
E-mail: lehrstuhl-2@oc.uni-stuttgart.de

Supporting information for this article is available on the WWW under https://doi.org/10.1002/cbic.202000678

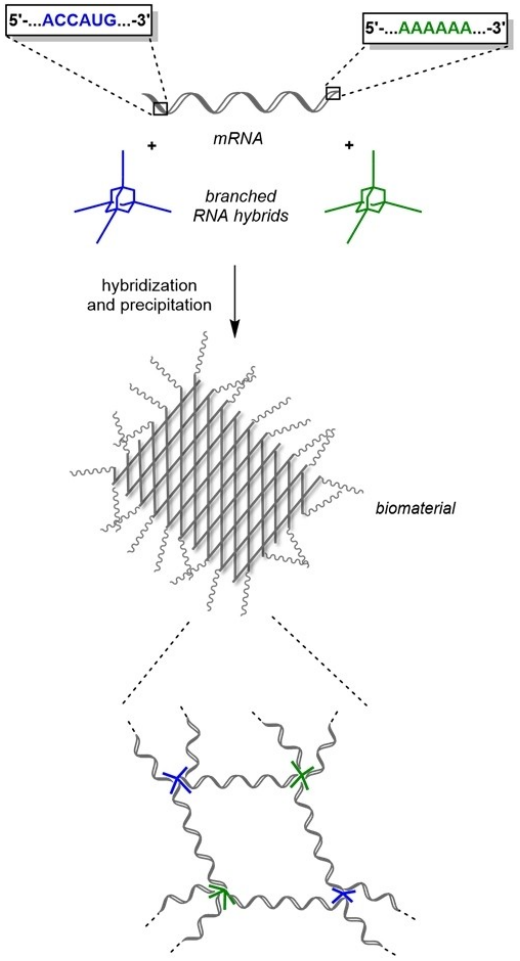

Figure 1. Assembly of mRNA (gray) and RNA hybrids (blue/green) into a hybridization network precipitating as a biomaterial. The sequences in the mRNA that are complementary to the hybrids are highlighted as inserts in the upper part of the graphic.

oligocations. Both hybrids are composed of unmodified RNA and an aliphatic alcohol as branching element, making them attractive as non-toxic alternatives to established formulation agents.

Results and Discussion

Scheme 1 shows the sequences of the two branched oligoribonucleotide hybrids prepared and the synthetic route employed, which use commercially available phosphoramidites. Either synthesis started from adamantane tetraol (**1**, dubbed "TOA"), which was reacted with a phosphoramidite building block of uridine for solid-phase RNA synthesis, using the TBDMS protocol. The aliphatic alcohol was considered unproblematic in terms of possible toxicity,[11] and the arms are entirely made up of unmodified RNA.

The synthetic protocols were optimized, using the conditions for solution-phase assembly of branched DNA hybrids[10] as starting point. Since the silyl-protected RNA building blocks are more lipophilic, the precipitation steps in particular, had to be adjusted, e.g. by using diisopropyl ether instead of MTBE. Table 1 gives an overview of the solvent mixtures and coupling times used, as well as the yield of crudes, as obtained after extractive work-up and precipitation. The first four-fold coupling produced tetranucleotide intermediate **2**, which was then used to elaborate the protected form of $(U)_6$TOA (**3**). Two-stage deprotection, first using basic conditions, and then using $3HF{\cdot}NEt_3$ to remove the silyl protecting groups, gave hybrid **4**, designed to hybridize to the poly(A) tails of mRNAs. Likewise, five coupling cycles with **2** and phosphoramidite building blocks for A, C, G and U gave protected intermediate **5**, which was deprotected to give mixed sequence hybrid **6**.

Conversion was confirmed by MALDI-TOF MS of crudes after each step. For the analyses, small samples were drawn and subjected to oxidation, detritylation, and basic deprotection with NH_4OH/methylamine (AMA) or ammonium hydroxide/ethanol, followed by mass spectrometry. Figure 2 shows a spectrum for intermediate **2**, and Figure 2b/2c show MALDI spectra for the full-size hybrids **4** and **6**.

The deprotected hybrids were purified by ion-exchange chromatography, using either HPLC (**4**) or chromatography at ambient pressure, using a pre-filled cartridge. Overall yields of isolated pure material were 6% for $(CAUGGU)_4$TOA (**6**) and 14% for $(UUUUUU)_4$TOA (**4**) over 20 steps (including coupling, oxidation, detritylation and final deprotection steps). Figure 3 shows ^{1}H NMR spectra of either of the hybrids thus prepared. We note that the hybrids were prepared by convenient

Table 1. Results for coupling cycles in the solution-phase synthesis of branched RNA hybrids.

Hybrid	Phosphoramidite[a]	Solvent ratio CH_3CN/DMF	Coupl. time [h]	Yield of crude [%][b]
$(U_{TBDMS})_4$TOA (**2**)	U	1.5/1	22	97
$(UU_{TBDMS})_4$TOA (**7**)	U	1.5/1	42	96
$(UUU_{TBDMS})_4$TOA (**8**)	U	1.3/1	42	88
$(UUUU_{TBDMS})_4$TOA (**9**)	U	1.3/1	48	93
$(UUUUU_{TBDMS})_4$TOA (**10**)	U	1.3/1	42	81
$(UUUUUU_{TBDMS})_4$TOA (**3**)	U	1.3/1	48	86
$(GU_{TBDMS})_4$TOA (**11**)	G	1.5/1	24	84
$(GGU_{TBDMS})_4$TOA (**12**)	G	1.5/1	20	81
$(UGGU_{TBDMS})_4$TOA (**13**)	U	1.5/1	43	73
$(AUGGU_{TBDMS})_4$TOA (**14**)	A	1.5/1	72	80
$(CAUGGU_{TBDMS})_4$TOA (**5**)	C	1.5/1	49	94

[a] 8 equiv. of phosphoramidite per coupling was used for the assembly of **4**, and 12 equiv. of the respective phosphoramidite per coupling step were used for **6**. [b] Yield of DMT-deprotected RNA hybrid after precipitation, determined by UV absorbance.

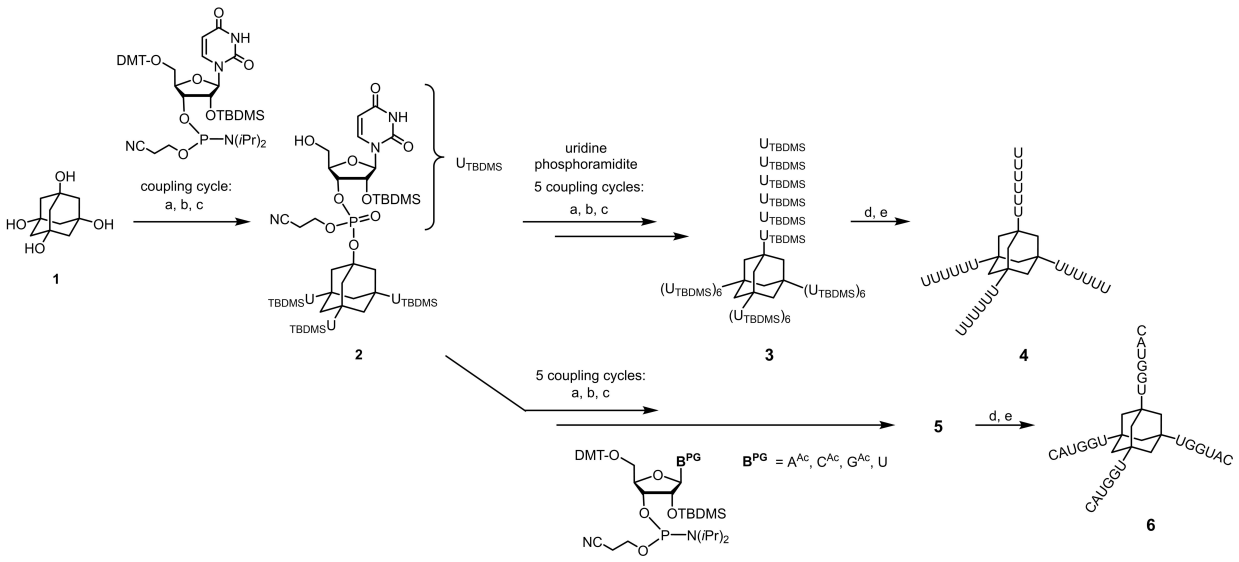

Scheme 1. Solution-phase synthesis of branched oligoribonucleotide hybrids starting from adamantane tetraol **1**·. a) Phosphoramidite building block for U, A, C, or G, tetrazole, DMF; b) *t*BuOOH; c) DCA/CH_2Cl_2; d) NH_4OH/ethanol (3:1) or AMA (25% NH_4OH/40% $MeNH_2$; 1:1); e) 3 HF·NEt_3.

solution-phase syntheses, without chromatography on any but the final stage. Double-digit milligram quantities were obtained for both **4** and **6** in single-run syntheses.

We then proceeded to testing the ability of the hybrids to induce formation of a biomaterial. For this, we used the mRNA encoding for the RAV–G protein of the rabies virus, kindly provided by CureVac.[34] The sequence of this mRNA, which is 1957 nucleotides in length, is provided in the SI. As mentioned above, hybrid **4** is complementary to the poly(A) tail, whereas the hexamer hybrid arms of **6** cover the start codon locus (Figure 1).

Material formation was tested with two different stoichiometries (equimolar and equimolar to the strands of the RNA arms), and three different mRNA/hybrid combinations (either hybrid alone or the combination of both). To monitor the hybridization-induced precipitation, the first experiments were carried out in a cuvette. At an mRNA concentration of 0.4 μM in 1 M NaCl-Tris buffer, the kinetics of Figure 4 were obtained. Even at this low concentration, either of the two hybrids induced precipitation of most of the mRNA. Biomaterial formation occurred slightly faster when RNA hybrids were employed at equimolar concentration, as compared to experiments with the same concentration of arms and mRNA (stoichiometry 1:4). When both of the hybrids were employed, precipitation was faster still, and up to 82% of the mRNA was captured in the material (Figure 4c). At the low concentration, the half-life time of the precipitation process was 16.8 h with hybrid **4**, 13.5 h with **6**, and 7.5 h with both hybrids at the equimolar ratio of mRNA/hybrids, as determined by monoexponential fits (R^2 values >0.96). Overall, differences in the precipitation kinetics were modest, though, suggesting that the principle of crosslinking-by hybridization is robust and not limited to a narrow range of stoichiometries or target loci in the mRNA. Control experiments with linear RNA strands of the same sequence showed no precipitation (Figure 4a), even after 40 h, suggesting that multivalent binding is the main cause for the formation of biomaterials.

Next, we performed biomaterial forming assays at 4 μM mRNA concentration in order to obtain larger quantities of the materials. Again, the RNA hybrids were incubated with the mRNA at two different stoichiometric ratios; equimolar or at a ratio of 4:1, so that every arm of hybrid **6** has one equivalent of its target sequence in the solution. Visible quantities of the biomaterial were observed within hours of incubation at 5 °C, and the extent of precipitation depicted in the upper parts of Figure 4 was reached after 3 d. In all samples containing both mRNA and hybrid(s), most of the mRNA had been precipitated at this time point, whereas the control experiments carried out in parallel showed no solid formation. The materials were then harvested, and their composition was analyzed by denaturing PAGE (Figure 5). At the concentration of these assays, little of the mRNA and RNA hybrids remained in the supernatant, as detected by electrophoresis (right-most lanes of gels in Figure 5).

Then, we performed a series of experiments using an additional ratio of mRNA to **4**/**6** of 4:4:1 at the mRNA concentration of 4 μM. The mRNA chosen for our study contains 64 adenosine nucleotides in its poly(A) tail, allowing the arms of hybrid **4** to hybridize more than once. We analyzed the biomaterials obtained by RP-HPLC to obtain quantitative data on their composition. Under the chromatographic conditions chosen, the hybrids and mRNA were well separated, but **4** and **6** co-migrated. The ratio between the two hybrids was then determined by quantitative MALDI-TOF mass spectrometry,[35] after calibration plots had established the differences of desorption/ionization efficiencies for the two analytes. Table 2 summarizes the results.

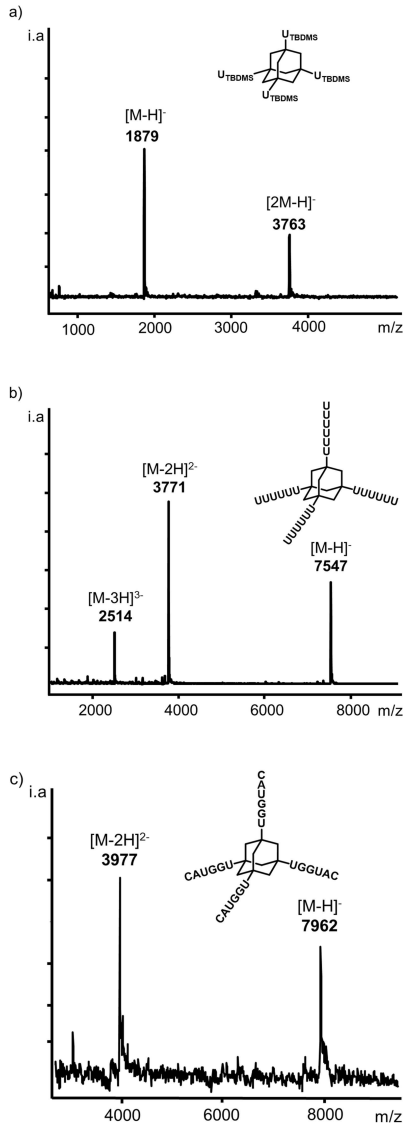

Figure 2. MALDI-TOF mass spectra of RNA hybrids. a) crude of intermediate $(U_{TBDMS})_6$TOA (**2**) after precipitation and basic deprotection with AMA; b) $(UUUUUU)_4$TOA (**4**), and c) $(CAUGGU)_4$TOA (**6**), as obtained after chromatography.

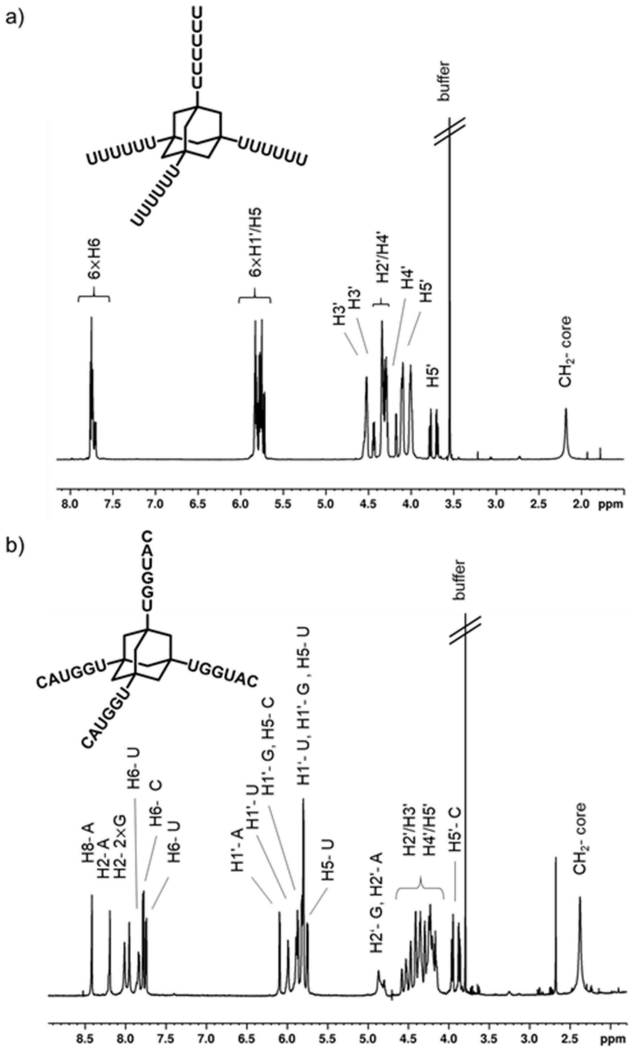

Figure 3. ^{1}H NMR spectra of RNA hybrids (D_2O, Tris buffer, 700 MHz). a) $(UUUUUU)_4$TOA (**4**) at 25 °C, b) $(CAUGGU)_4$TOA (**6**) at 40 °C.

At either of the molar ratios tested ≥95% of the mRNA was found in the biomaterial confirming the near-quantitative incorporation detected by PAGE. The branched RNA hybrids were recovered in 67 to 76% of the amount employed in the respective assay, and the ratio of the RNA hybrids to each other was in favor of hybrid **4**, which can bind to the mRNA more than once. Finally, the molar ratios determined by UV absorbance confirmed that one RNA hybrid was able to bind more than one mRNA molecule.

Exploratory experiments using dynamic light scattering indicated that particles in the size range of 100–1000 nm are formed in the assembly process (Figures S12–S14, SI). Further, a

Table 2. Composition of biomaterials composed of mRNA and RNA hybrids, as detected by HPLC analysis.[a]

Starting ratio mRNA/**4**/**6**	mRNA found [%][b]	Hybrids **4** + **6** found [%][b]	Ratio **4**/**6** in material[c]
4:4:4	95	76	1.6:1
4:4:1	96	67	3.7:1
4:1:1	98	75	1.3:1

[a] Materials were obtained by annealing 4 μM mRNA with 4 μM or 1 μM of each hybrid in buffer containing 1 M NaCl, pH 7.1 from 70 °C to 4 °C in 2 h, followed by 4 °C for 72 h. After harvesting by centrifugation for 1 min at 2000 *g*, materials were denatured by treating with deionized water and heating to 60 °C and analyzed by RP-HPLC at 55 °C column temperature. [b] As determined from UV absorbances of HPLC fractions. [c] As determined by MALDI-TOF spectrometry, using conditions for quantitative detection[35] with correction for differences in desorption/ionization efficiency.

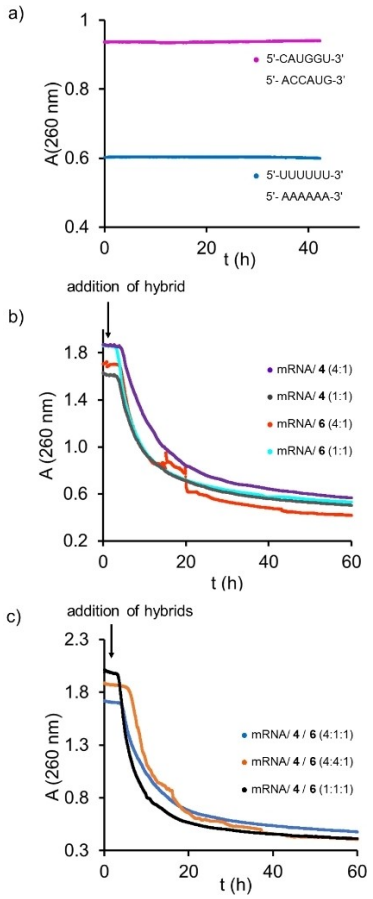

Figure 4. Kinetics of biomaterial formation from mRNA (0.4 μM) and RNA hybrids, as detected by decrease of UV-absorption at 260 nm. a) Control experiment with linear complementary RNA strands; b) mRNA with one hybrid only at different hybrid concentrations, as expressed by molar ratios; c) mRNA plus both hybrids (**4** + **6**) at the different hybrid concentrations. Experiments were performed in duplicate. See Figure S10 of the SI for an overlay of data. Conditions: 1 M NaCl, 10 mM Tris, pH 7.1, 5 °C.

first set of exploratory experiments on the release of the mRNA from the hybridization networks with our hybrids was performed. For this, biomaterial was formed by annealing 0.4 μM mRNA with 0.4 μM hybrids (**4**/**6**) at 1 M NaCl in a cuvette, followed by incubation for 16 h at 4 °C and centrifugation. The supernatant was removed, and Tris buffer containing a near-physiological concentration of NaCl (150 mM) was added, and the solution was warmed from 4 °C to 50 °C at a rate 0.5 °C/min without stirring. The release into the solution occurred at or a little above body temperature (Figure 6).

Material formation through multivalent hybridization of the arms of branched DNA hybrids alone, or in combination with connector duplexes featuring sticky ends, has been reported before.[5–12] The underlying multivalent hybridization events usually require shorter duplex lengths than those of linear strands, so that dinucleotides can suffice to induce assembly into a material.[5] Even in light of these earlier findings, the current results are surprising. One surprising aspect is that precipitation sets in without the addition of divalent cations, such as Mg^{2+} salts. This is crucial, as di- and trivalent cations can catalyze the hydrolysis of RNA, affecting the stability of formulations. Further, with adamantane tetraol, a very small aliphatic branching element was used, lacking the rigid aromatic side chain spacers that can engage in hydrophobic interactions that may dominate over hybridization.[9] Finally, RNA, rather than DNA arms were used, so that the entire biomaterial contains nothing but RNA and the small tetraol core.

In our current design, the change to a branching element less prone to assemble by itself than the larger lipophilic cores of previous DNA hybrids[5–9] combined with an mRNA hybridization partner offering just a few, distant binding loci was "compensated" by extending the arms from dimers[5,6] to hexamers. The robust assembly process observed speaks for the design and for the concept of multivalent binding as a means to achieve strong interactions,[36] even for nucleic acids. The difference in the hybridization properties of the G/C-free $(U_6)_4$TOA (**4**) and the more strongly pairing $(CAUGGU)_4$TOA (**6**) in control experiments with linear strands is in agreement with hybridization as the predominant mode of interaction with target strands. Under the experimental conditions chosen, the weakly pairing **4** does not show hypochromicity when treated with $(A)_6$, whereas **6** with its C/G-containing mixed sequence does, when treated with complementary strands (Figure S11, SI). In the biomaterial, **4** can bind multiple times to the poly(A) tail of the mRNAs, whereas **6** has but one preferred binding site that is fully complementary. The local extent of non-covalent crosslinking is probably different for the two hybrids, with some compensating effects, but the cooperative transition observed in the UV-monitored melting experiment (Figure 6) suggests that they act synergistically in forming a hybridization network. The new biomaterial thus prepared has the potential to rival other macromolecular materials, such as hydrogels,[37,38,39] in terms of practical applications. As briefly mentioned above, practical applications for RNA-containing materials may include vaccination,[13–24] gene-based therapies,[25] and the manipulation of cellular phenotypes.[26]

Conclusions

Genetic material that does not carry the risk of being inserted into the patient genome, and that can be designed to induce the expression of specific proteins, such as mRNA, is a most valuable tool in therapy.[27,33] To achieve the desired effect *in vivo*, the RNA has to be formulated. This is no easy task for a well soluble class of linear, polyanionic biopolymers. The results presented here establish that the formation of a biomaterial can be induced without resorting to cationic compounds. Rather, little RNA "snippets", if properly arranged in dendritic fashion, suffice to compel mRNA to assembly into networks that precipitate from dilute, pH neutral aqueous solution devoid of divalent cations, lipids or other toxicologically problematic components. From the resulting biomaterial, the mRNA is readily released intact under mild conditions. Our results also show how the "RNA snippet" constructs can be synthesized in convenient solution phase chain assembly protocols, using

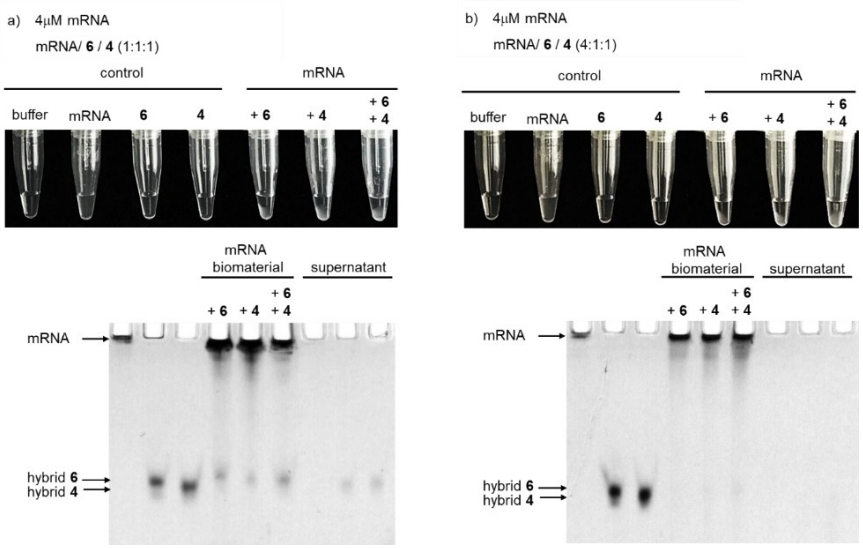

Figure 5. Formation of a biomaterial by hybridization of RNA hybrids to mRNA at different molar ratios. In the upper part of each figure photographs of assay vessels are shown for 4 μM mRNA in 10 mM Tris buffer, 1 M NaCl, pH 7.1 after 3 d at 5 °C. In the lower part of each figure, denaturing PAGE gels (10%, 7 M urea) of samples from the same biomaterial-forming assays are shown. For this, materials were dissolved in deionized water containing 40% formamide by heating to 80 °C and the resulting solution was applied in the respective pocket of the gel. a) Material-forming assay with a molar ratio mRNA to RNA hybrid(s) (**4**/**6**) of 1 : 1(:1). b) The same assay with a molar ratio mRNA to RNA hybrid(s) (**4**/**6**) of 4 : 1(:1). The gels were analyzed by UV shadowing. See Figure S9 of the SI for an agarose gel in which the mRNA gives distinct bands.

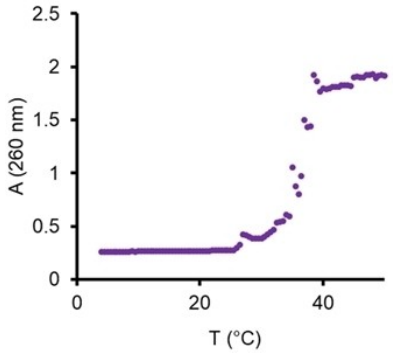

Figure 6. Release of mRNA from biomaterial at body temperature. A sample of mRNA biomaterial prepared from mRNA and hybrids **4** + **6**, was treated with buffer of near-physiological salt concentration and warmed from 4–50 °C at a rate of 0.5 °C/min. The release of the mRNA was monitored by UV absorbance at 260 nm. In the absence of stirring, local density gradients leading to small maxima in the curve are expected. The final absorbance corresponds to approx. 70% of the initial mRNA employed in the formulation process.

inexpensive, commercial RNA building blocks. By combining the power of organic synthesis, the use of a simple aliphatic alcohol as branching element, and the approach to induce a desired biological effect with designed RNA sequences, the avenue work opens a new avenue for achieving vaccination and therapy with mRNA and opens the door for biomedical studies that realize this potential.

Acknowledgements

The authors thank CureVac AG (Tübingen) for a donation of mRNA samples and for performing the particle size measurements (H. Maart). We thank Dr. P. Baumhof, Dr. A. Schwenger and Dr. P. Tremmel for discussions, and Helmut Griesser for a review of the manuscript. This work was supported by Deutsche Forschungsgemeinschaft grant No. RI 1063 15-1 and CRC TRR 235, project P6. Open access funding enabled and organized by Projekt DEAL.

Conflict of Interest

The authors declare no conflict of interest.

Keywords: biomaterial · hybridization · mRNA networks · RNA hybrids · vaccines

[1] A. Schwenger, H. Griesser, C. Richert, in: *DNA in Supramolecular Chemistry and Nanotechnology* (Eds.: E. Stulz, G. Clever), Wiley, Chichester, **2015**, ISBN: 9781118696866.
[2] R. Elghanian, J. J. Storhoff, R. C. Mucic, R. L. Letsinger, C. A. Mirkin, *Science* **1997**, *277*, 1078–1081.
[3] K. M. Stewart, L. W. McLaughlin, *J. Am. Chem. Soc.* **2004**, *126*, 2050–2057.
[4] J. Zimmermann, M. P. J. Cebulla, S. Mönninghoff, G. von Kiedrowski, *Angew. Chem. Int. Ed.* **2008**, *47*, 3626–3630; *Angew. Chem.* **2008**, *120*, 3682–3686.
[5] M. Meng, C. Ahlborn, M. Bauer, O. Plietzsch, S. A. Soomro, A. Singh, T. Muller, W. Wenzel, S. Bräse, C. Richert, *ChemBioChem* **2009**, *10*, 1335–1339.
[6] A. Singh, M. Tolev, M. Meng, K. Klenin, O. Plietzsch, C. I. Schilling, T. Muller, M. Nieger, S. Bräse, W. Wenzel, C. Richert, *Angew. Chem. Int. Ed.* **2011**, *50*, 3227–3231; *Angew. Chem.* **2011**, *123*, 3285–3289.

[7] A. Singh, M. Tolev, C. Schilling, S. Bräse, H. Griesser, C. Richert, *J. Org. Chem.* **2012**, *77*, 2718–2728.
[8] H. Griesser, M. Tolev, A. Singh, T. Sabirov, C. Gerlach, C. Richert, *J. Org. Chem.* **2012**, *77*, 2703–2717.
[9] A. Schwenger, C. Gerlach, H. Griesser, C. Richert, *J. Org. Chem.* **2014**, *79*, 11558–11566.
[10] A. Schwenger, N. Birchall, C. Richert, *Eur. J. Org. Chem.* **2017**, *39*, 5852–5864.
[11] H. Griesser, A. Schwenger, C. Richert, *ChemMedChem* **2017**, *12*, 1759–1767.
[12] A. Schwenger, T. P. Jurkowski, C. Richert, *ChemBioChem* **2018**, *19*, 1–9.
[13] H. S. Hong, S. D. Koch, B. Scheel, U. Gnad-Vogt, A. Schröder, K. Knallen, V. Wiegand, L. Backert, O. Kohlbacher, I. Hoerr, M. Fotin-Mleczek, J. M. Billingsley, *Oncoimmunology* **2016**, *5*, e1249560. DOI: 10.1080/2162402X.2016.1249560.
[14] M. Sebastian, A. Schröder, B. Scheel, H. S. Hong, A. Muth, L. von Boehmer, A. Zippelius, F. Mayer, M. Reck, D. Atanackovic, M. Thomas, F. Schneller, J. Stöhlmacher, H. Bernhard, A. Gröschel, T. Lander, J. Probst, T. Strack, V. Wiegand, U. Gnad-Vogt, K. Kallen, I. Hoerr, F. von der Muelbe, M. Fotin-Mleczek, A. Knuth, S. D. Koch, *Cancer Immunol. Immunother.* **2019**, *68*, 799–812.
[15] A. Papachristofilou, M. M. Hipp, U. Klinkhardt, M. Früh, M. Sebastian, C. Weiss, M. Pless, R. Cathomas, W. Hilbe, G. Pall, T. Wehler, J. Alt, H. Bischoff, M. Geißler, F. Griesinger, K. Kallen, M. Fotin-Mleczek, A. Schröder, B. Scheel, A. Muth, T. Seibel, C. Stosnach, F. Doener, H. S. Hong, S. D. Koch, U. Gnad-Vogt, A. Zippelius, *J. Immunother. Cancer* **2019**, *7*, 38.
[16] C. R. Stadler, H. Bähr-Mahmud, L. Celik, B. Hebich, A. S. Roth, R. P. Roth, K. Karikó, Ö. Türeci, U. Sahin, *Nat. Med.* **2017**, *23*, 815–817.
[17] S. Rauch, E. Jasny, K. E. Schmidt, B. Petsch, *Front. Immunol.* **2018**, *9*, 1–24.
[18] F. Doener, H. S. Hong, I. Meyer, K. Tagjalli-Mehr, A. Daehling, R. Heidenreich, S. D. Koch, M. Fotin- Mleczek, U. Gnad-Vogt, *Vaccine* **2019**, *37*, 1819–1826.
[19] S. Sabnis, E. Sathyajith Kumarasinghe, T. Salerno, C. Mihai, T. Ketova, J. J. Senn, A. Lynn, A. Bulychev, I. McFadyen, J. Chan, Ö. Almarsson, M. G. Stanton, K. E. Benenato, *Mol. Ther.* **2018**, *26*, 1509–1519.
[20] M. A. Monslow, S. Elbashir, N. L. Sullivan, D. S. Thiriot, P. Ahl, J. Smith, E. Miller, J. Cook, S. Cosmi, E. Thoryk, M. Citron, N. Thambi, C. Shaw, D. Hazuda, K. A. Vora, *Vaccine* **2020**, *38*, 5793–5802.
[21] N. Pardi, M. J. Hogan, R. S. Pelc, H. Muramatsu, H. Andersen, C. R. DeMaso, K. A. Dowd, L. L. Sutherland, R. M. Scearce, R. Parks, W. Wagner, A. Granados, J. Greenhouse, M. Walker, E. Willis, J. Yu, C. E. McGee, G. D. Sempowski, B. L. Mui, Y. K. Tam, Y. Huang, D. Vanlandingham, V. M. Holmes, H. Balachandran, S. Sahu, M. Lifton, S. Higgs, S. E. Hensley, T. D. Madden, M. J. Hope, K. Karikó, S. Santra, B. S. Graham, M. G. Lewis, T. C. Pierson, B. F. Haynes, D. Weissman, *Nature* **2017**, *543*, 248–251.
[22] M. J. Mulligan, K. E. Lyke, N. Kitchin, J. Absalon, A. Gurtman, S. Lockhart, K. Neuzil, V. Raabe, R. Bailey, K. A. Swanson, P. Li, K. Koury, W. Kalina, D. Cooper, C. Fontes-Garfias, P. Shi, Ö. Türeci, K. R. Tompkins, E. E. Walsh, R. Frenck, A. R. Falsey, P. R. Dormitzer, W. C. Gruber, U. Şahin, K. U. Jansen, *Nature* **2020**, https://doi.org/10.1038/s41586-020-2639-4.
[23] K. S. Corbett, D. K. Edwards, S. R. Leist, et al., *Nature* **2020**, https://doi.org/10.1038/s41586-020-2622-0.
[24] K. S. Corbett, et al., *New Engl. J. Med.* **2020**, *383*, 1544–1555. DOI: 10.1056/NEJMoa2024671.
[25] H. Yin, R. L. Kanasty, A. A. Eltoukhy, A. J. Vegas, J. R. Dorkin, D. G. Anderson, *Nat. Rev. Genet.* **2014**, *15*, 541–555.
[26] E. S. Quabius, G. Krupp, *Nat. Biotechnol.* **2015**, *32*, 229–235.
[27] M. A. Islam, E. K. G. Reesor, Y. Xu, H. R. Zope, B. R. Zetter, J. Shi, *Biomater. Sci.* **2015**, *3*, 1519–1533.
[28] G. Tavernier, O. Andries, J. Demeester, N. N. Sanders, S. C. De Smedt, J. Rejman, *J. Controlled Release* **2011**, *150*, 238–247.
[29] K. Koji, N. Yoshinaga, Y. Mochida, T. Hong, T. Miyazaki, K. Kataoka, K. Osada, H. Cabral, S. Uchida, *Biomaterials* **2020**, *261*, 120332.
[30] R. W. Malone, P. L. Felgner, I. M. Verma, *Proc. Natl. Acad. Sci. USA* **1989**, *86*, 6077–6081.
[31] S. Van Meirvenne, L. Straetman, C. Heirman, M. Dullaers, C. De Greef, V. Van Tendeloo, K. Thielemans, *Cancer Gene Ther.* **2002**, *9*, 787–797.
[32] M. D. Mattozzi, M. J. Voges, P. A. Silver, J. C. Way, *J. Vis. Exp.* **2014**, *86*, e51234. DOI: 10.3791/51234.
[33] N. T. Jarzebska, S. Lauchli, C. Iselin, L.-E. French, P. Johansen, E. Guenova, T. M. Kündig, S. Pascolo, *Drug Delivery* **2020**, *1*, 1231–1235.
[34] M. Fotin-Mleczek, R. Heidenreich (CureVac), WO 2015/149944 A2, **2015**.
[35] D. Sarracino, C. Richert, *Bioorg. Med. Chem. Lett.*, **1996**, *6*, 2543–2548.
[36] M. Mammen, S. Choi, G. M. Whitesides, *Angew. Chem. Int. Ed. Engl.* **1998**, *37*, 2754–2794.
[37] F. Li, J. Tanng, J. Geng, D. Luo, D. Yang, *Prog. Polym. Sci.* **2019**, *98*, 101163.
[38] J. Tang, C. Yao, S. Jung, D. Luo, D. Yang, *Angew. Chem. Int. Ed.* **2020**, *59*, 2490–2495.
[39] C. Yao, H. Tang, W. Wu, J. Tang, W. Guo, D. Luo, D. Yang, *J. Am. Chem. Soc.* **2020**, *142*, 3422–3429.

Manuscript received: September 30, 2020
Revised manuscript received: October 21, 2020
Accepted manuscript online: October 26, 2020
Version of record online: November 18, 2020